



# Subsonic Potential Aerodynamics for Complex Configurations: A General Theory

LUIGI MORINO\*

*Boston University, Boston, Mass.*

AND

CHING-CHIANG KUO†

*NASA Ames Research Center, Moffett Field, Calif.*

A general theory of subsonic potential aerodynamic flow around a lifting body having arbitrary shape and motion is presented. By using the Green function method, an integral representation for the velocity potential is obtained for both supersonic and subsonic flow. Under small perturbation assumption, the potential at any point,  $P$ , in the field depends only upon the values of the potential and its normal derivative on the surface,  $\Sigma_B$ , of the body. On the surface of the body, this representation reduces to an integro-differential equation relating the potential and its normal derivative (which is known from the boundary conditions) on the surface  $\Sigma_B$ . The theory is applied to finite-thickness wings in subsonic steady and oscillatory flows. Comparison with existing results indicates that the method compares favorably with existing ones for both accuracy and computer time.

## Nomenclature

$a_\infty$	= freestream speed of sound
$b$	= span of wing
$b_k$	= Equation (20)
$c$	= chord of wing
$C_p$	= pressure coefficient
$C_l$	= lift distribution coefficient, $C_{p,l} - C_{p,u}$
$c_{ki}$	= Equation (21)
$F$	= nonlinear terms in Eq. (1)
$G$	= Green function, Eq. (4)
$h$	= thickness of wing
$k$	= reduced frequency, $\omega L/U_\infty$
$L$	= characteristic length
$M$	= Mach number, $U_\infty/a_\infty$
$\mathbf{n}$	= normal to surface in $x, y, z$ space
$\mathbf{N}$	= normal to surface in $X, Y, Z$ space
$NX, NY$	= number of elements in $X, Y$ directions
$r_\beta$	= Equation (5)
$R$	= Equation (12)
$S$	= function describing the surface $\Sigma$
$t$	= time
$T$	= nondimensional time, $a_\infty t/\beta L$
$x, y, z$	= space coordinates
$X, Y, Z$	= Prandtl-Glauert coordinates, Eq. (10)
$U_\infty$	= freestream velocity
$\beta$	= $(1 - M_\infty^2)^{1/2}$
$\theta$	= Equation (6)
$\sigma$	= surface surrounding body and wake in $x, y, z$ space
$\Sigma$	= surface surrounding body and wake in $X, Y, Z$ space
$\Sigma_B$	= surface surrounding body in $X, Y, Z$ space
$\tau$	= thickness ratio
$\Phi$	= velocity potential, $U_\infty(x + \phi)$
$\phi$	= perturbation velocity potential
$\phi_i$	= value of $\phi$ at the centroid of the element $\Sigma_i$
$\phi^{(n)}$	= normal derivative of $\phi$
$\omega$	= frequency of oscillation
$\Omega$	= $\omega L/\beta a_\infty$

$[ ]^0$	= $[ ]_{t_1=t-\theta}$
$( )_1$	= dummy variable of integration
$D/Dt$	= total time derivative, $\partial/\partial t + \nabla\Phi \cdot \nabla$

## I. Introduction

THE problem of evaluating the pressure distribution on a wing, in steady or oscillatory motion, in subsonic or supersonic flow, is a fundamental problem in aeroelasticity. This problem is usually solved by using well known lifting-surface theories.<sup>1-3</sup> These theories have two main disadvantages: first, they are numerically complex and hence time consuming and, second, they cannot be easily extended to cover more general problems (wing-body-tail interaction, helicopter blades, etc.).

An excellent analysis of the present state-of-the-art in the wing-body interaction problem is given by Ashley and Rodden.<sup>4</sup> A very short, by no means complete, review of potential flow around arbitrary configurations is given here. The methods of Rubbert and Saaris,<sup>5</sup> Labrujere, Loeve, and Sloof,<sup>6</sup> Hess and Smith,<sup>7,8</sup> Tulinius,<sup>9</sup> and Djojodihardjo and Widnall<sup>10</sup> use various combinations of sources and doublets inside and/or on the surface of the body. These methods are valid for steady subsonic flow except for the last one<sup>10</sup> which is valid for unsteady incompressible flow. Other methods, such as the one of Woodward<sup>11</sup> (for steady subsonic and supersonic flow) and of Kalman, Rodden, and Giesing<sup>12</sup> (for unsteady subsonic flow) use lifting surface elements and axial singularity distributions. The method of Giesing, Kalman, and Rodden<sup>13</sup> uses lifting-surface and slender-body theories combined with the method of images. This method applies to unsteady subsonic flows. Finally, in supersonic flow the methods of Woodward,<sup>11</sup> Baals, Robins, and Harris,<sup>14</sup> Shrout<sup>15</sup>, and Kariappa and Smith<sup>16</sup> should be mentioned.

A general theory of the unsteady compressible potential flow around lifting bodies having arbitrary configurations and motions is presented in Refs. 17 and 18. Applications to finite thickness wings in subsonic flow are given in Refs. 19-21. This paper summarizes the results presented in Refs. 18 and 21. For simplicity, only the subsonic flow is discussed; similar theoretical results obtained for supersonic flow are given in Refs. 17 and 18. The basic tool employed in the theory is the Green function method. As is well known, applying the Green function method for the wave equation yields the Huygens' Principle (or Kirchhoff's formula), which is the Green theorem for the wave equation

Received January 11, 1973; revision received August 27, 1973. This work was supported by NASA Langley Research Center under NASA Grant NGR 22-004-030. The authors wish to express their appreciation to E. C. Yates Jr., technical advisor of the program, for the stimulating discussions and invaluable suggestions made in connection with this work.

Index category: Nonsteady Aerodynamics.

\* Associate Professor of Aerospace Engineering. Member AIAA.

† NRC Postdoctoral Research Associate. Member AIAA.

(see Ref. 22, p. 501). The theory presented here is a generalization of the Huygens' Principle to the equation of the aerodynamic potential in a frame of reference traveling at velocity  $U_\infty$  with respect to the undisturbed air. In addition, there are cases (such as helicopter blades or spinning missiles, for instance) in which the surface of the aircraft cannot be assumed to be fixed with respect to the frame of reference, even when this is traveling at velocity  $U_\infty$  with respect to the undisturbed air. Hence, the surface  $\sigma$  (surrounding body and wake) is assumed to be moving with respect to the frame of reference.

## II. Formulation of the Problem

The perturbation velocity potential  $\phi$  for a flow having free-stream velocity  $U_\infty$  in the direction of the positive  $x$ -axis is given by

$$\nabla^2 \phi - (1/a_\infty^2)[\partial/\partial t + U_\infty \partial/\partial x]^2 \phi = F \quad (1)$$

where  $F$  is the contribution of the nonlinear terms. Let the surface of the body be described in the general form<sup>‡</sup>

$$S(x, y, z, t) = 0 \quad (2)$$

Then the boundary conditions on the body are given by  $DS/Dt = 0$  or

$$\phi^{(n)} \equiv \frac{\partial \phi}{\partial n} \equiv \frac{\nabla S}{|\nabla S|} \cdot \nabla \phi = -\frac{1}{U_\infty |\nabla S|} \left( \frac{\partial S}{\partial t} + U_\infty \frac{\partial S}{\partial x} \right) \quad (3)$$

In order to solve this problem, it is convenient to transform it into an integral equation. Consider the Green function of the linearized equation of the subsonic potential

$$G = -(1/4\pi r_\beta) \delta(t_1 - t + \theta) \quad (4)$$

where  $\delta$  is the Dirac delta function and

$$r_\beta = \{(x_1 - x)^2 + \beta^2[(y_1 - y)^2 + (z_1 - z)^2]\}^{1/2} \quad (5)$$

$$\theta = (1/a_\infty^2 \beta) [M(x_1 - x) + r_\beta] \quad (6)$$

The generalized Huygens' Principle derived in Ref. 17 by using the classical Green theorem method is given by

$$4\pi E \phi(x, y, z, t) = - \iint_{\Sigma^\theta} \left[ \nabla_1 S \cdot \nabla_1 \phi - \frac{1}{a_\infty^2} \frac{dS}{dt_1} \frac{d\phi}{dt_1} \right] \frac{1}{r_\beta} \frac{d\sigma^\theta}{|\nabla_1 S^\theta|} + \iint_{\Sigma^\theta} \left[ \nabla_1 S \cdot \nabla_1 \left( \frac{1}{r_\beta} \right) - \frac{1}{a_\infty^2} \frac{dS}{dt_1} \frac{d}{dt_1} \left( \frac{1}{r_\beta} \right) \right] [\phi]^\theta \frac{d\sigma^\theta}{|\nabla_1 S^\theta|} - \frac{\partial}{\partial t} \iint_{\Sigma^\theta} \left[ \nabla_1 S \cdot \nabla_1 \theta - \frac{1}{a_\infty^2} \frac{dS}{dt_1} \left( 1 + U_\infty \frac{\partial \theta}{\partial x_1} \right) \right] [\phi]^\theta \frac{1}{r_\beta} \frac{d\sigma^\theta}{|\nabla_1 S^\theta|} - \iiint_{-\infty}^{\infty} [EF]^\theta (1/r_\beta) dV_1 \quad (7)$$

where  $d/dt_1 = \partial/\partial t_1 + U_\infty \partial/\partial x_1$ , and

$$\begin{aligned} E &= 0 \quad \text{inside } \sigma \\ E &= \frac{1}{2} \quad \text{on } \sigma \\ E &= 1 \quad \text{outside } \sigma \end{aligned} \quad (8)$$

and  $[\ ]^\theta$  indicates evaluation at  $t_1 = t - \theta$ . Similarly,  $\sigma^\theta$  is the surface given by

$$S^\theta \equiv S(x_1, y_1, z_1, t - \theta) = 0 \quad (9)$$

where  $(x_1, y_1, z_1)$  is the dummy point of integration on  $\sigma^\theta$ . If initial conditions are prescribed, Eq. (7) should be modified as indicated in Appendix F of Ref. 17.

It should be noted that if the point is on the hypersurface  $S = 0$ , Eq. (7) yields an integro-differential equation which may be used for evaluating the value of  $\phi$  on the surface. The contribution of the nonlinear terms, if not negligible, may be obtained by successive approximations or by asymptotic expansions (singular perturbation methods). It may be noted that Eq. (7) is very general since it is valid even if the surface of the body is moving in time with respect to the frame of reference (helicopter blades, spinning missiles, etc.). However,

<sup>‡</sup> For convenience, the arbitrary multiplicative sign in Eq. (2) is chosen so that  $\nabla S$  has the direction of the outwardly directed normal  $\mathbf{n}$ .

even if the nonlinear terms are negligible, the solution of Eq. (7) is quite cumbersome, hence possible simplifications are described in the following. In many practical applications, one deals with small perturbation flow around surfaces with negligible motion with respect to the frame of reference. In this case, the surface  $\sigma^\theta$  can be replaced by the time-independent surface  $\sigma$  given by  $S(x, y, z) = 0$ . The term  $\partial S/\partial t$  will be retained only in the boundary conditions. Then, neglecting the nonlinear terms and introducing the generalized Prandtl-Glauert transformation

$$X = x/\beta L, \quad Y = y/L, \quad Z = z/L, \quad T = a_\infty \beta t/L \quad (10)$$

where  $L$  is a characteristic length of the body, Eq. (7) reduces to

$$4\pi E \phi(X, Y, Z, T) = - \iint_{\Sigma} \left[ \frac{\partial \phi}{\partial N_1} \right]^\Theta \frac{1}{R} d\Sigma + \iint_{\Sigma} \frac{\partial}{\partial N_1} \left( \frac{1}{R} \right) [\phi]^\Theta d\Sigma - \iint_{\Sigma} \frac{\partial R}{\partial N_1} \frac{1}{R} \left[ \frac{\partial \phi}{\partial T} \right]^\Theta d\Sigma \quad (11)$$

where  $\Theta = a_\infty \beta \theta/L = M(X_1 - X) + R$ ,  $\mathbf{N}$  is the normal to the surface  $\Sigma$  of the space  $X, Y, Z$  and

$$R = [(X_1 - X)^2 + (Y_1 - Y)^2 + (Z_1 - Z)^2]^{1/2} \quad (12)$$

Finally, neglecting terms of the same order of magnitude as the nonlinear terms,  $\partial \phi/\partial N$  can be replaced by  $\partial \phi/\partial n$ , which is known from the boundary conditions, Eq. (3).

Further simplification is obtained for the problem of harmonic oscillations (with frequency  $\omega$ ) about a fixed configuration. In this case, introducing the complex potential  $\hat{\phi}$  such that

$$\phi(X, Y, Z, T) = \hat{\phi}(X, Y, Z) e^{i\Omega(T + M X)} \quad (13)$$

and neglecting higher order terms in the boundary conditions, Eq. (11) reduces to

$$4\pi E \hat{\phi}(X, Y, Z) = - \iint_{\Sigma} \hat{\phi}^{(n)} \frac{e^{-i\Omega R}}{R} d\Sigma + \iint_{\Sigma} \hat{\phi} \frac{\partial}{\partial N_1} \left( \frac{e^{-i\Omega R}}{R} \right) d\Sigma \quad (14)$$

with

$$\hat{\phi}^{(n)} = \phi^{(n)} e^{-i\Omega(T + M X)} \quad (15)$$

In Eq. (13),  $\Omega$  is the compressible reduced frequency and  $\Omega = \omega L/a_\infty \beta = kM/\beta$ .

In summary, for oscillatory subsonic flow, the solution can be obtained from Eq. (14) in which the surface is assumed to be time-independent (except for the boundary conditions) and the effects of higher order terms in the differential equation, Eq. (1), and the boundary conditions have been neglected. As previously mentioned, these effects can be obtained eventually by perturbation methods, which are now being explored.

It may be noted that, as already mentioned, if the point  $X, Y, Z$  is outside  $\Sigma$ , Eq. (14) is an integral representation of the potential  $\hat{\phi}$  in terms of the values of  $\hat{\phi}$  and  $\hat{\phi}^{(n)}$  on the surface  $\Sigma$ . On the other hand, if the point  $X, Y, Z$  is on  $\Sigma$ , Eq. (14) is a two-dimensional Fredholm integral equation of second kind relating the unknown values of  $\hat{\phi}$  on  $\Sigma$  to the known values of  $\hat{\phi}^{(n)}$ . Once this equation has been solved by some approximate method, Eq. (14) itself can be used to evaluate  $\phi$  as well as its derivatives (perturbation velocity components) anywhere in the flowfield. Finally, using the Bernoulli theorem the pressure can also be evaluated.

It should be noted that if the thickness of the body approaches zero (thin wings, for instance) the term which contains the boundary condition vanishes. This implies that for very thin wings the integral equation is near singular. Hence, the formulation proposed here would not be complete unless the question of existence and uniqueness is analyzed. Also, the treatment of the wake and the Kutta condition should be considered. Thus, in order to study the feasibility, the method was applied to the worst possible case, that is, very thin wings. For, if the method works for thin wings, it can be safely assumed to be valid for more complex configurations as well. § Hence, only the numerical

§ Recent results, obtained for complex configurations in subsonic and supersonic, steady and oscillatory flow, confirmed the conclusions anticipated here.

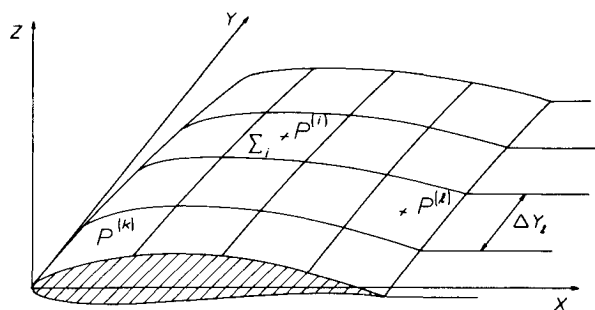


Fig. 1 Geometry of problem: elements and control points.

results necessary to discuss the near-singular behavior for small thickness are presented here. First, the numerical formulation used for obtaining the results is summarized. For simplicity, only the steady-state formulation is given here. The extension to oscillatory flow is outlined in the Appendix.

### III. Numerical Procedure

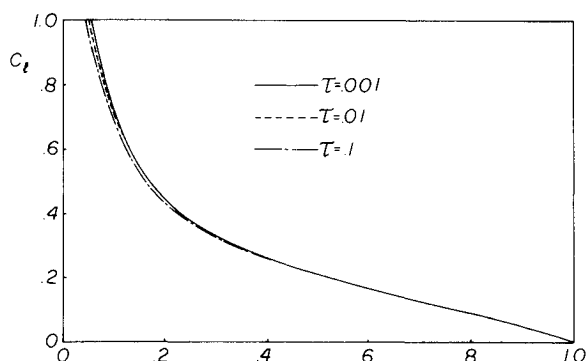
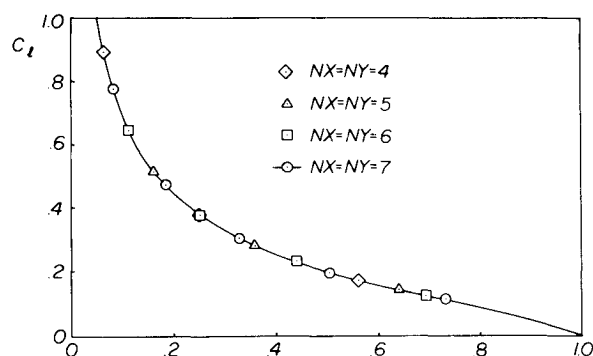
If the point  $X, Y, Z$  is on  $\Sigma$ ,  $E = \frac{1}{2}$ , and Eq. (14), for steady flow, reduces to

$$\phi(X, Y, Z) = -\frac{1}{2\pi} \iint_{\Sigma} \phi^{(n)} \frac{1}{R} d\Sigma + \frac{1}{2\pi} \iint_{\Sigma} \phi \frac{\partial}{\partial N_1} \left( \frac{1}{R} \right) d\Sigma \quad (16)$$

It should be noted that, if  $\phi^{(n)}$  is known everywhere on  $\Sigma$ , Eq. (16) is a Fredholm integral equation of second kind, whose solution exists and is unique (solution of the external Neumann's problem for the Laplace equation). However, the branch of the surface  $\Sigma$ , surrounding the wake, is not known. A finite element representation of a wake is possible<sup>10,23</sup> but unnecessary here. Hence, the simplified procedure used in Ref. 17 is summarized here. The wake is assumed to be composed of straight vortex lines emanating from the trailing edge and parallel to the direction of the undisturbed flow. Since the pressure is continuous across the wake,  $\Delta\phi \equiv \phi_u - \phi_l$  is constant along a vortex line and equal to its value,  $\Delta\phi_{TE}$ , at the trailing edge. Noting that the source contribution of the wake is equal to zero, Eq. (16) reduces to

$$\phi(X, Y, Z) = -\frac{1}{2\pi} \iint_{\Sigma_B} \phi^{(n)} \frac{1}{R} d\Sigma + \frac{1}{2\pi} \iint_{\Sigma_B} \phi \frac{\partial}{\partial N_1} \left( \frac{1}{R} \right) d\Sigma + \frac{1}{2\pi} \int_{TE} \Delta\phi_{TE} \left[ (Y_1 - Y) \frac{\partial Z_{TE}}{\partial Y_1} - (Z_{TE} - Z) \right] dY_1 \int_{X_{TE}}^{\infty} \frac{1}{R^3} dX_1 \quad (17)$$

where  $\Sigma_B$  is the surface of the body and  $\int_{TE}$  indicates the integration along the trailing edge. The integral with respect to  $X_1$  is evaluated analytically as

Fig. 2 Lift distribution coefficients at root elements for  $NX = NY = 4$ .Fig. 3 Lift distribution coefficients at root elements for  $\tau = 0.001$ .

$$I_w = \int_{X_{TE}}^{\infty} \frac{1}{R^3} dX_1 = \frac{1}{(Y_1 - Y)^2 + (Z_{TE} - Z)^2} \left[ 1 - \frac{X_{TE} - X}{R_{TE}} \right] \quad (18)$$

Except for a few special cases, Eq. (17) must be solved by using some approximate numerical method. The one used here was chosen mainly because of its flexibility (for wing-body-tail interaction, for instance). The surface  $\Sigma_B$  is divided into  $N$  small finite surface elements,  $\Sigma_i$ , see Fig. 1. The potential  $\phi$  is assumed to be constant within each element and equal to the value  $\phi_i$  at the centroid of the element. Then, by satisfying Eq. (17) at the centroid of each element, one obtains a system of  $N$  linear equations and  $N$  unknowns

$$\phi_k = b_k + \sum_{i=1}^N c_{ki} \phi_i + \sum_{i=1}^N w_{ki} \phi_i \quad (k = 1, 2, \dots, N) \quad (19)$$

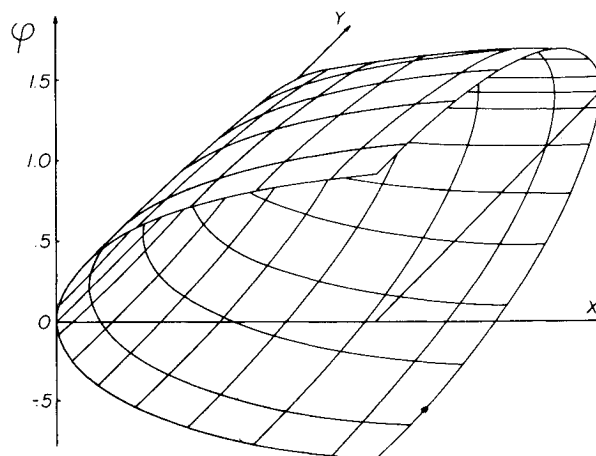
where

$$b_k = -\iint_{\Sigma_B} \phi^{(n)} \frac{1}{2\pi R_k} d\Sigma \quad (20)$$

and

$$c_{ki} = \iint_{\Sigma_i} \frac{\partial}{\partial N_1} \left( \frac{1}{2\pi R_k} \right) d\Sigma_i \quad (21)$$

In Eqs. (20) and (21),  $R_k$  is the distance of the centroid of the element  $\Sigma_k$  from the dummy point of integration. The coefficients  $c_{ki}$  are evaluated analytically by assuming that the element  $\Sigma_i$  is replaced by its tangent plane at the centroid. A similar procedure is used for  $b_k$ . The analytical expressions for the evaluation of  $c_{ki}$  and  $b_k$  are given in Appendix E of Ref. 17 for tangent-plane elements having trapezoidal planforms. Finally, the coefficients,  $w_{ki}$ , which represent the contribution of the wake, are obtained as follows. The value of  $\Delta\phi_{TE}$  is assumed to be equal to the value  $\Delta\phi$  evaluated at the centroids of the elements in contact with the

Fig. 4 Potential distribution for  $\tau = 0.001$  and  $NX = NY = 7$ .

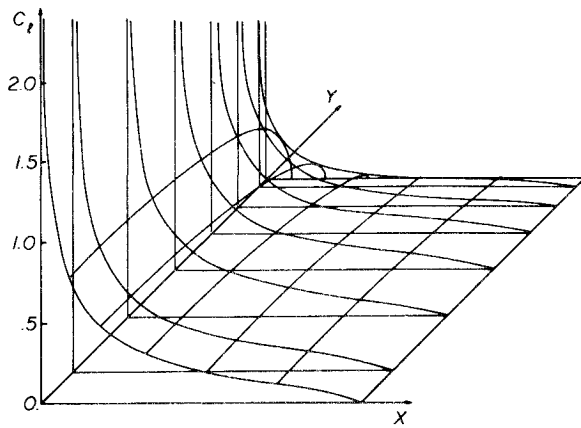


Fig. 5 Lift distribution coefficient for  $\tau = 0.001$  and  $NX = NY = 7$ .

trailing edge: this assumption is reasonable in view of the Kutta condition that the pressure difference vanishes at the trailing edge. Hence, the coefficients  $w_{ki}$  are given by

$$w_{ki} = \pm \frac{1}{2\pi} \int_{\Delta Y_i} \left[ (Y_1 - Y) \frac{\partial Z_{TE}}{\partial Y_1} - (Z_{TE} - Z) \right] I_w dY_1 \quad (22)$$

for the elements,  $\Sigma_i$ , in contact with the trailing edge, and  $w_{ki} = 0$  otherwise. In Eq. (22), the upper (lower) sign holds for the upper (lower) surface of the wing.

It may be worth noting that the aforementioned is the only use made of the Kutta condition. This seems to be a consequence of the discrete formulation of the problem (see for instance, Ref. 8, pp. 35–45). It may be noted, however, that if the unknowns are assumed to be the values of  $\phi$  at the corner of the elements, the Kutta condition must be imposed, since for a control point at the trailing edge, only one equation is available (the ones for the upper and lower sides being identical) for two unknowns,  $\phi_{u,TE}$  and  $\phi_{l,TE}$ .

#### IV. Numerical Results

Equation (19) can be solved numerically. However, as previously anticipated, if the thickness of the wing goes to zero, the operator of Eq. (17) becomes singular and correspondingly, the determinant of Eq. (19) becomes equal to zero.<sup>17</sup> This implies that the proposed theory has a limitation. For, if the thickness ratio is too small, the determinant is very close to zero and strong elimination of significant figures is expected. Hence, in order to study the feasibility of the method, Eq. (19) has been

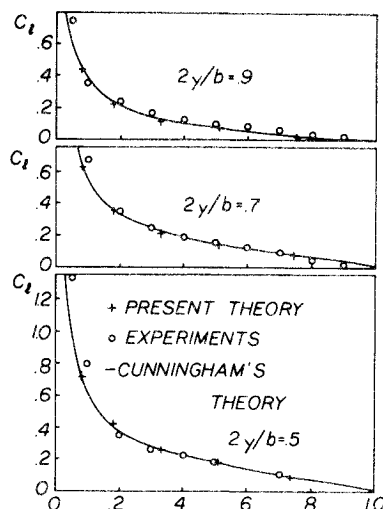


Fig. 6 Comparison to experimental and theoretical results for  $\tau = 0.001$  and  $NX = NY = 7$ .

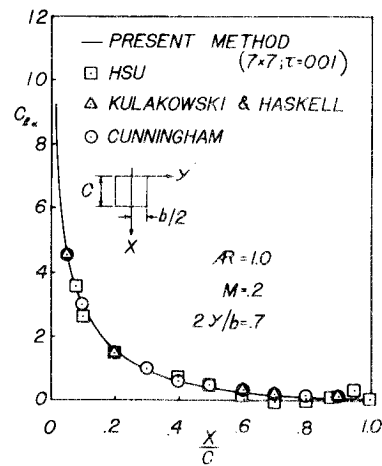


Fig. 7 Lift coefficient for a rectangular wing.

solved numerically for wings having thickness ratios as close as possible to zero. Typical results are presented here.

The wing geometry at zero angle-of-attack is given by

$$\begin{aligned} x &= x_{LE} + c(\eta)\xi \\ y &= (b/2)\eta \\ z &= \pm \tau c(0)^{3/4} (3)^{1/2} (\xi)^{1/2} (1 - \xi)(1 - \eta^2)^{1/2} \end{aligned} \quad (23)$$

where  $c$  is the chord and  $b$  is the span of the wing. In order to compensate for the square-root behavior of the potential at the leading edge and the tip of the wing, the transformation

$$\xi = \bar{X}^2 \quad \eta = 1 - (1 - \bar{Y})^2 \quad (24)$$

was introduced. Surface elements with projections in the  $\bar{X}$ ,  $\bar{Y}$  plane of constant size

$$\Delta \bar{X} = 1/NX \quad \Delta \bar{Y} = 1/NY \quad (25)$$

( $NX$  and  $NY$  are the number of elements in  $\bar{X}$  and  $\bar{Y}$  direction, on half wing) were used. The centroid is the center of element in the  $\bar{X}$ ,  $\bar{Y}$  plane. Finally, the lift distribution coefficient,  $C_l$ , is evaluated as

$$C_l = 2(\partial/\partial \bar{X})(\phi_u - \phi_l)d\bar{X}/dx \quad (26)$$

where  $d\bar{X}/dx = 1/(2c\bar{X})$  and the derivative with respect to  $\bar{X}$  is evaluated by finite difference.

It should be noted that the transformation, Eq. (24), although convenient (to improve the rate of convergence and for the evaluation of the pressure coefficient), is not essential to the problem. Also, as previously mentioned, the pressure can be evaluated from the value of the velocity obtained by differentiating the integral representation for  $\phi$ . Hence, Eq. (26), although convenient, is not essential to the method. A feasibility analysis is present in Figs. 2–6 for a rectangular wing with aspect ratio  $R = 3$ , angle-of-attack  $\alpha = 5^\circ$  and Mach number  $M = 0.24$ . The effect of the thickness is shown in Fig. 2 where  $C_l$  is the

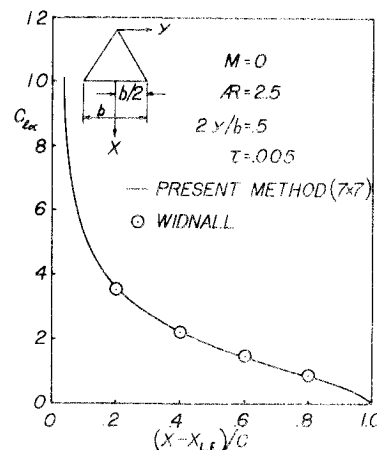
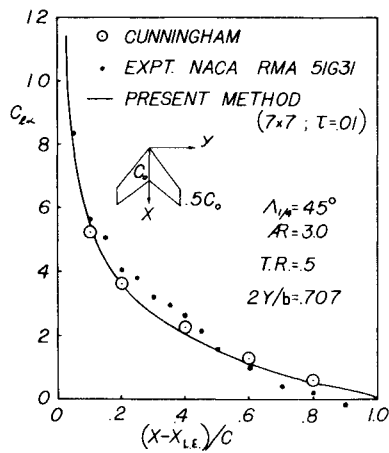


Fig. 8 Lift coefficient for a delta wing.

Fig. 9 Lift coefficient for a tapered wing.



lift distribution coefficient. As previously mentioned, this analysis is important because it shows that the method is feasible despite the anticipated elimination of significant figures: no claim is made here that Fig. 2 indicates the thickness effect on  $C_p$ , since this is affected by nonlinear terms. For the same reason, only pressure difference (instead of pressure distribution) is examined here. The analysis of convergence is presented in Fig. 3. The velocity potential  $\phi$  and the lift distribution coefficient  $C_l$  over the wing are given in Figs. 4 and 5, while a comparison with existing experimental<sup>24</sup> and theoretical<sup>25</sup> results is shown in Fig. 6.

Other results for wings in steady state are presented in Figs. 7–10. In Fig. 7, the results for a rectangular wing of aspect ratio  $AR=1$  at  $M=0.2$  are compared to the ones of Hsu,<sup>26</sup> Kulakowski and Haskell,<sup>27</sup> and Cunningham,<sup>25</sup> whereas in Fig. 8, the results for a delta wing with  $AR=2.5$  and  $M=0$  are compared to the ones obtained by Widnall.<sup>28</sup> Finally in Fig. 9, a tapered wing of  $AR=3$ , taper ratio  $T.R.=0.5$  and  $M=0.8$  are compared with the theoretical results of Cunningham<sup>25</sup> and the experimental ones of Kolbe and Boltz.<sup>29</sup>

In Fig. 10, the section lift coefficients  $C_L$  (which are generally more significant than the pressure distribution, since small error on  $C_p$  near the leading edge may yield large errors on  $C_l$ ) are compared to the values obtained by Yates<sup>30</sup> for a rectangular wing with  $AR=4$  and  $M=0.507$ .

Results for oscillating wings are presented in Figs. 11–15. Figures 11–13 present the results for a rectangular wing with aspect ratio  $AR=2$ ,  $M=0$  and reduced frequency  $k=\omega c/U_\infty=2$ , rigidly oscillating around the axis  $x=c/2$ . Figure 11 presents the analysis of convergence and Fig. 12 the thickness effect. These confirm the results obtained for the steady-state problems that the convergence is very fast and that the thickness effect is very small. In Fig. 13, the results are compared to the ones obtained by Laschka.<sup>31</sup>

Figures 14 and 15 present the results for a rectangular wing with aspect ratio  $AR=3$ , oscillating in a bending mode described by<sup>3,24</sup>

Fig. 10 Section lift coefficient  $C_L$  for rectangular wing.

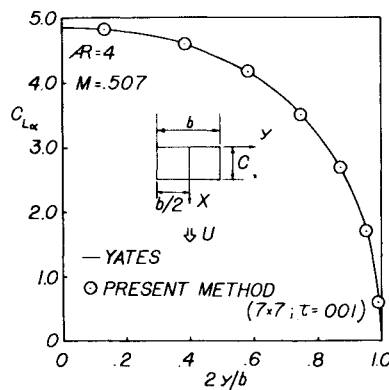
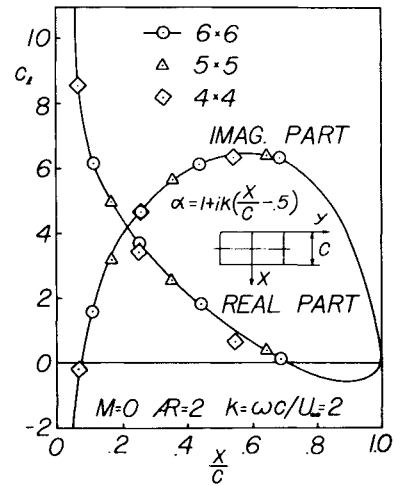


Fig. 11 Analysis of convergence:  $C_l$  at root elements for a rectangular wing oscillating around axis  $x=c/2$  ( $\tau=0.001$ ).



$$z = 0.18043 |y/s| + 1.70255 |y/s|^2 - 1.13688 |y/s|^3 + 0.25387 |y/s|^4 \quad (27)$$

where  $s$  is the semispan of the wing. The results (for  $M=0.24$  and  $k=\omega c/2U_\infty=0.47$  and thickness ratio  $\tau=0.005$ ) are normalized by dividing by the velocity of the wing at the tip. The results are compared to the ones obtained by Lessing et al.,<sup>24</sup> and Albano and Rodden.<sup>3</sup>

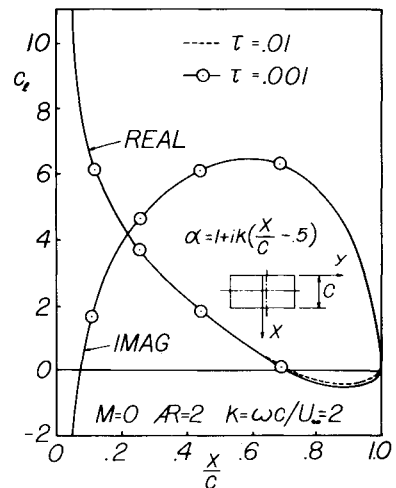
In conclusion, if one takes into account the fact that the numerical formulation is still very crude, the results presented above indicate that the agreement of the present method with existing results is surprisingly good. More refined numerical formulations are now being explored.

## V. Conclusions

A general theory for steady and unsteady, subsonic flows around complex configurations has been developed and applied to finite-thickness wings, for steady and oscillatory flows.

The results obtained indicate that the method is accurate even for very small thickness ratios (good results were obtained even for thickness ratio  $\tau=1/1000$ , although some elimination of significant figures was encountered). Furthermore, the computer time was surprisingly small: for steady state it ranges from 13 sec for  $NX=NY=4$ , to 128 sec for  $NX=NY=7$ , while for unsteady state it goes from 39 sec for  $NX=NY=4$ , to 159 sec for  $NX=NY=6$ . These results were obtained on the IBM 360/50 at Boston University. An advantage was taken of symmetry with respect to the  $y$ -axis and antisymmetry with respect to the  $z$ -axis. Applications to complex configurations

Fig. 12 Effect of thickness for rectangular wing oscillating around axis  $x=c/2$  ( $NX=NY=7$ ).



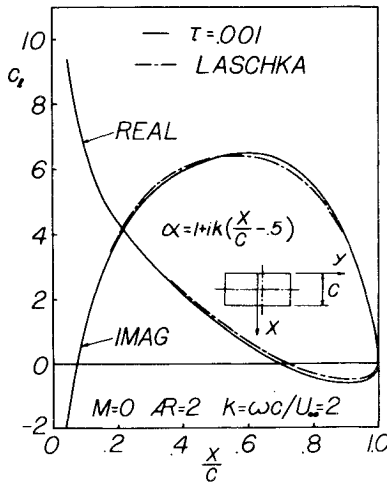


Fig. 13 Rectangular wing oscillating around axis  $x = c/2$ :  $C_l$  at  $\eta = 0.15$  ( $NX = NY = 7$ ,  $\tau = 0.001$ ).

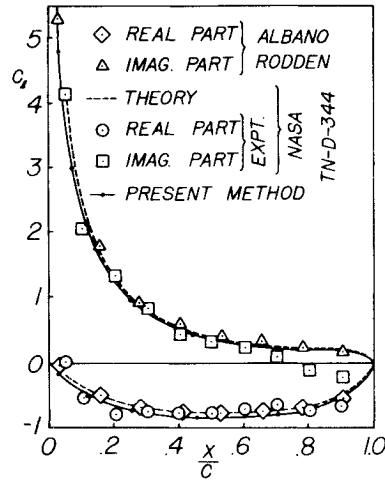


Fig. 15 Rectangular wing oscillating in bending mode ( $AR = 3$ ,  $M = 0.24$ ,  $k = 0.47$ ):  $C_l$  at  $\eta = 0.9$ .

are now under way and the results obtained thus far indicate similar conclusions. In summary, the method has a very broad applicability since it is accurate, fast and can cover subsonic steady and unsteady flow around complex configurations.

Finally, it may be worth adding a few comments about alternative numerical formulations which can be used in connection with the theoretical results, Eq. (7), presented here. Again, for the sake of simplicity, the discussion is carried out for the steady incompressible case. Consider first the normal derivative of the basic equation

$$\frac{\partial \phi}{\partial n} = \iint_{\Sigma} \phi^{(n)} \frac{\partial}{\partial n} \left( \frac{-1}{4\pi R} \right) d\Sigma - \iint_{\Sigma} \phi \frac{\partial^2}{\partial n \partial n_1} \left( \frac{-1}{4\pi R} \right) d\Sigma \quad (28)$$

By taking the limit as the control approaches  $\Sigma$ , one obtains an integral equation, different from Eq. (16), which has the advantage that if the thickness is equal to zero, the operator is not singular; the limit equation is the one used by Haviland.<sup>32</sup>

Two other alternative formulations are obtained by introducing a convenient flowfield inside the surface  $\Sigma$  (see Lamb,<sup>22</sup> pp. 58–61). If the value of the potential is continuous across the surface, one obtains

$$\phi = \iint_{\Sigma} S \frac{1}{4\pi R} d\Sigma \quad (29)$$

where  $S$  is the intensity of the source distribution (equal to the discontinuity in normal velocity). On the other hand, if the normal velocity is continuous across the surface, then one obtains

$$\phi = \iint_{\Sigma} D \frac{\partial}{\partial n_1} \left( \frac{1}{4\pi R} \right) d\Sigma \quad (30)$$

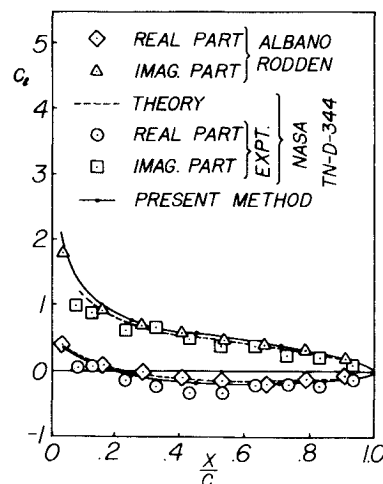


Fig. 14 Rectangular wing oscillating in bending mode ( $AR = 3$ ,  $M = 0.24$ ,  $k = 0.47$ ):  $C_l$  at  $\eta = 0$ .

where  $D$  is the intensity of the doublet distribution (equal to the discontinuity of  $\phi$ ). By taking the normal derivative of Eqs. (29) and (30) and imposing the boundary conditions, one obtains two integral equations for the unknowns  $S$  and  $D$ , respectively. These methods are used, for instance, by Hess and Smith<sup>7</sup> and Djodjodhardjo and Widnall,<sup>10</sup> respectively. It may be noted that more complex formulations can be obtained by combining two or more of these four basic methods, Eqs. (17, 28–30). The advantages and disadvantages of the four basic methods are briefly discussed here. Note first that the “source method,” Eq. (29), is limited to nonlifting bodies: extensions to lifting configurations must include doublet distributions as well.<sup>8</sup> On the other hand, the other two methods, Eqs. (28) and (30), if applied to a closed surface, involve a singular operator (which yields a determinant equal to zero). For, outside  $\Sigma$

$$\iint_{\Sigma} \frac{\partial}{\partial n_1} \left( \frac{1}{4\pi R} \right) d\Sigma = -\frac{1}{4\pi} \iint_{\Sigma} d\Omega = 0 \quad (31)$$

(where  $\Omega$  represents the solid angle<sup>17</sup>) and thus its normal derivative is zero: hence, Eqs. (28) and (30) have a nontrivial (constant) solution for the homogeneous problem.¶ Thus, the method presented here is the only one of the four basic methods, which can be applied to “closed-surface” description of lifting configurations. On the other hand, as previously mentioned, combinations of two or more of the four basic methods can be usefully employed. Various combinations are now being explored.

## VI. Appendix A

The numerical formulation for subsonic oscillatory flows is outlined in this Appendix. Starting from Eq. (14), with  $E = \frac{1}{2}$ , and using the same procedure described in the main body of this paper, one obtains an equation of the type of Eq. (19) where now

$$b_k = \iint_{\Sigma} \hat{\phi}^{(n)} \frac{e^{-i\Omega R_k}}{2\pi R_k} d\Sigma - \sum_{i=1}^N [\hat{\phi}^{(n)} e^{-i\Omega R_k}]_{P=P^{(i)}} \iint_{\Sigma_i} \frac{1}{2\pi R_k} d\Sigma_i \quad (A1)$$

$$c_{ki} = - \iint_{\Sigma_i} \frac{\partial}{\partial N_1} \left( \frac{e^{-i\Omega R_k}}{2\pi R_k} \right) d\Sigma_i \simeq - [e^{-i\Omega R_k} (1 + i\Omega R_k)]_{P=P^{(i)}} \iint_{\Sigma_i} \frac{\partial}{\partial N_1} \left( \frac{1}{2\pi R_k} \right) d\Sigma_i \quad (A2)$$

where the integrals are equal to the steady-state case and are evaluated in the same way. Finally, the expression for  $w_{ki}$  is still the same except for Eq. (18) which is replaced by<sup>17,21</sup>

¶ It should be noted however, that these two methods can be used for open surfaces (lifting surfaces<sup>32</sup>), or for the analysis of the transient response.<sup>10</sup>

$$I_w = (Z - Z_1) e^{i(\Omega/M)(X_{TE} - X)} \left\{ \frac{\Omega\beta}{MR_0} \left[ K_1(\kappa) + \frac{\pi i}{2} I_1(\kappa) \right] + \frac{X - X_1}{R_0^2} e^{i\Omega[(X - X_1)/M] - R} + \frac{1}{R_0^2} F \left( \frac{MR + X_1 - X}{\beta R_0} \right) \right\}_{X=X_{TE}} \quad (A3)$$

where  $R_0 = [(Y_1 - Y)^2 + (Z_1 - Z)^2]^{1/2}$ ,  $\kappa = \Omega\beta R_0/M$  and  $I_1$  and  $K_1$  are the modified Bessel functions of first order of first and second kind, respectively. Finally, the function  $F$  is given by

$$F(u) = \sum_{n=1}^{\infty} F_n(u) \quad (A4)$$

where  $F_n$  can be evaluated by using the recurrent formula

$$F_n(u) = \frac{1}{n!} (-i)^n \kappa^n (1 + u^2)^{1/2} u^{n-1} + \frac{\kappa^2}{n(n-2)} F_{n-2}(u) \quad (A5)$$

with

$$F_1(u) = -i\kappa(1 + u^2)^{1/2} \quad (A6)$$

$$F_2(u) = -\frac{\kappa^2}{2} \{u(1 + u^2)^{1/2} - \ln[u + (1 + u^2)^{1/2}]\}$$

Note that <sup>17</sup> for  $Z = Z_1$ ,  $I_w$  yields a closed form representation of the classical Kernel function of Ref. 33.

## References

- Ashley, H., Widnall, S., and Landahl, M. T., "New Directions in Lifting Surface Theory," *AIAA Journal*, Vol. 3, No. 1, Jan. 1965, pp. 3-16.
- Landahl, M. T. and Stark, V. J. E., "Numerical Lifting-Surface Theory—Problems and Progress," *AIAA Journal*, Vol. 6, No. 11, Nov. 1968, pp. 2049-2060.
- Albano, E. and Rodden, W. P., "A Doublet-Lattice Method for Calculating Lift Distribution on Oscillating Surfaces in Subsonic Flows," *AIAA Journal*, Vol. 7, No. 2, Feb. 1969, pp. 279-285.
- Ashley, H. and Rodden, W. P., "Wing-Body Aerodynamic Interaction," *Annual Review of Fluid Mechanics*, Vol. 4, 1972, pp. 431-472.
- Rubbert, P. E. and Saaris, G. R., "Review and Evaluation of a Three-Dimensional Lifting Potential Flow Analysis Method for Arbitrary Configurations," AIAA Paper 72-188, San Diego, Calif., 1972.
- Labrujere, T. E., Loeve, W., and Slooff, J. W., "An Approximate Method for the Calculation of the Pressure Distribution on Wing-Body Combinations at Subcritical Speeds," AGARD Conference Proceedings 71, Aerodynamic Interference, Sept. 1970.
- Hess, J. L., and Smith, A. M. O., "Calculation of Potential Flow About Arbitrary Bodies," *Progress in Aeronautical Sciences*, Vol. 8, Pergamon Press, New York, 1966.
- Hess, J. L., "Calculation of Potential Flow About Arbitrary Three-Dimensional Lifting Bodies," Rept. MDC-J5679-01, Oct. 1972, Douglas Aircraft Co., Long Beach, Calif.
- Tulinus, J. R., "Theoretical Prediction of Thick Wing and Pylon-Fanpod-Nacelle Aerodynamic Characteristics at Subcritical Speeds," Rept. NA-71-447, June 1971, North American Rockwell Corp., El Segundo, Calif.
- Djojodihardjo, R. H. and Widnall, S. E., "A Numerical Method for the Calculation of Nonlinear Unsteady Lifting Potential Flow Problems," *AIAA Journal*, Vol. 7, No. 10, Oct. 1969, pp. 2001-2009.
- Woodward, F. A., "Analysis and Design of Wing-Body Combinations at Subsonic and Supersonic Speeds," *Journal of Aircraft*, Vol. 5, No. 6, Nov.-Dec. 1968, pp. 528-534.
- Kalman, T. P., Rodden, W. P., and Giesing, J. P., "Application of the Doublet-Lattice Method to Nonplanar Configurations in Subsonic Flow," *Journal of Aircraft*, Vol. 8, No. 6, June 1971, pp. 406-413.
- Giesing, J. P., Kalman, T. P., and Rodden, W. P., "Subsonic Steady and Oscillatory Aerodynamics for Multiple Interfering Wings and Bodies," *Journal of Aircraft*, Vol. 9, No. 10, Oct. 1972, pp. 693-702.
- Baals, D. D., Robins, A. W., and Harris, R. V., Jr., "Aerodynamic Design Integration of Supersonic Aircraft," *Journal of Aircraft*, Vol. 7, No. 5, Sept.-Oct. 1970, pp. 385-394.
- Shrout, B. L., "Extension of a Numerical Solution for the Aerodynamic Characteristics of a Wing to Include a Canard or Horizontal Tail," AGARD Conference Proceedings 71, Aerodynamic Interference, Sept. 1970.
- Kariappa and Smith, B. C. C., "Development and Applications of Supersonic Unsteady Consistent Aerodynamics for Interfering Parallel Wings," AIAA Paper 73-317, Williamsburg, Va., 1973.
- Morino, L., "Unsteady Compressible Potential Flow Around Lifting Bodies Having Arbitrary Shapes and Motions," TR-72-01, June 1972, Boston Univ., Boston, Mass.
- Morino, L., "Unsteady Compressible Potential Flow Around Lifting Bodies: General Theory," AIAA Paper 73-196, Washington, D.C., 1973.
- Kuo, C. C. and Morino, L., "Steady Subsonic Flow Around Finite-Thickness Wings," TR-73-02, Feb. 1973, Boston Univ., Boston, Mass.
- Morino, L. and Kuo, C. C., "Unsteady Subsonic Flow Around Oscillating Finite-Thickness Wings," TR-73-03, Feb. 1973, Boston Univ., Boston, Mass.
- Morino, L. and Kuo, C. C., "Unsteady Subsonic Compressible Flow Around Finite-Thickness Wings," AIAA Paper 73-313, Williamsburg, Va., 1973.
- Lamb, Sir H., *Hydrodynamics*, 6th ed., Dover, New York, 1945, pp. 58-61.
- Mangler, K. W. and Smith, J. H. B., "Behaviour of the Vortex Sheet at the Trailing Edge of a Lifting Wing," *The Aeronautical Journal of the Royal Aeronautical Society*, Vol. 74, Nov. 1970, pp. 906-908.
- Lessing, H. C., Troutman, J. C., and Menees, G. P., Experimental Determination of the Pressure Distribution on a Rectangular Wing Oscillating in the First Bending Mode for Mach Numbers from 0.24 to 1.30," TN D-344, 1960, NASA.
- Cunningham, A. M., Jr., "An Efficient, Steady Subsonic Collocation Method for Solving Lifting-Surface Problems," *Journal of Aircraft*, Vol. 8, No. 3, March 1971, pp. 168-176.
- Hsu, P. T., "Flutter of Low Aspect-Ratio Wings, Part I, Calculation of Pressure Distributions for Oscillating Wings of Arbitrary Platform in Subsonic Flow by the Kernel-Function Methods," TR-64-1, Oct. 1957, MIT, Cambridge, Mass.
- Kulakowski, L. J. and Haskell, R. N., "Solution of Subsonic Nonplanar Lifting-Surface Problems by Means of High-Speed Digital Computers," *Journal of Aerospace Sciences*, Vol. 28, Feb. 1961, pp. 103-113.
- Ashley, H. and Landahl, M., *Aerodynamics of Wings and Bodies*, Addison-Wesley, Reading, Mass., 1965, p. 159.
- Kolbe, C. D. and Boltz, F. W., "The Forces and Pressure Distribution at Subsonic Speeds on a Planar Wing Having 45° of Sweep Back, an Aspect Ratio of 3, and a Taper Ratio of 0.5," RMA51G31, Oct. 1951, NACA.
- Yates, E. C., Jr., private communication, April 1971, Boston, Mass.
- Laschka, B., "Die Instationären Luftkräfte an Harmonisch Schwingenden Tragflügeln Endlicher Spannweite Bei Unter-Und Überschallgeschwindigkeit," *Jahrbuch*, 1961, der WGL, pp. 207-219.
- Haviland, J. K., "Downwash-Velocity Potential Method for Lifting Surfaces," *AIAA Journal*, Vol. 9, No. 11, Nov. 1971, pp. 2268-2269.
- Watkins, C. E., Runyan, H. S., and Woolston, D. S., "On the Kernel Function of the Integral Equation Relating the Lift and Downwash Distributions of Oscillating Finite Wings in Subsonic Flow," Rept. 1234, 1955, NACA (supersedes NACA TN 3131).